Electronic Supplementary Material (ESI) for Chemical Communications.

Supplementary Information

Engineering of CdS-chain arrays assembled through S···S interactions in 1D semiconductive coordination polymers

Asuka Nishibe,[a] Ryohei Akiyoshi,*[a] Akinori Saeki,[b] Kazuyoshi Ogasawara,[a] Takaaki Tsuruoka [c] and Daisuke Tanaka*[a]

[a] Department of Chemistry, School of Science, Kwansei Gakuin University, 1 Gakuen Uegahara, Sanda, Hyogo 669-1330, Japan

[b] Department of Applied Chemistry, Graduate School of Engineering, Osaka University, 2-1 Yamadaoka, Suita, Osaka 565-0871, Japan

[c] Department of Nanobiochemistry, Frontiers of Innovative Research in Science and Technology (FIRST), Konan University, Kobe, Hyogo 650-0047, Japan

Table of Contents

Experimental

Experimental Procedures

Materials

$Cd(NO_3)_2 \cdot 4H_2O$ (98%) were purchased from Sigma-Aldrich. *o*-Methoxybenzenethiol (*o*-HSPhOMe) (>98.0 %), *m*-Methoxybenzenethiol (*m*-HSPhOMe) (>98.0 %), and *p*-Methoxybenzenethiol (*p*-HSPhOMe) (>96.0 %) were purchased from Tokyo Chemical Industry Co. Toluene (≥99.0 %), *N,N*-dimethylformamide (DMF) (≥99.5 %), propylamine ($Pr\text{-}NH_2$) (≥98.0 %) and acetone (≥99.0 %) were purchased from FUJIFILM Wako Pure Chemical Industries. All chemicals and solvents were of reagent grade and were used without further purification.

Synthesis

Single crystals of **KGF-29**.

Single crystals of **KGF-29** were obtained using dimerized *o*-HSPhOMe formed through disulfide bonds based on the previously reported procedure.[S1] $Cd(NO_3)_2 \cdot 4H_2O$ (18.5 mg, 0.06 mmol) and dimerized *o*-HSPhOMe (16.7 mg, 0.12 mmol) were mixed in $Pr\text{-}NH_2/H_2O$/toluene (2 mL; v/v = 2:1:3). The solution was heated at 100 °C for 96 h in a sealed autoclave and cooled to 30 °C over 12 h to yield **KGF-29** as colorless needle-like crystals. In this synthetic scheme, Cd(II) ions are assumed to act as a Lewis acid to weaken the disulfide bond of dimerized *o*-HSPhOMe, while $Pr\text{-}NH_2$ acts as a reductant to produce anionic $SPhOMe^-$ monomers.

Single crystals of **KGF-30**

$Cd(NO_3)_2 \cdot 4H_2O$ (23.1 mg, 0.08 mmol) and *m*-HSPhOMe (21.5 mg, 0.15 mmol) were dissolved in H_2O/DMF (2 mL; v/v = 1:1). The solution was heated at 80 °C for 48 h in a sealed autoclave and cooled to 30 °C over 12 h to yield **KGF-30** as colorless needle-like crystals.

Single crystals of **KGF-31**

$Cd(NO_3)_2 \cdot 4H_2O$ (74.0 mg, 0.24 mmol) and *p*-HSPhOMe (70.1 mg, 0.48 mmol) were dissolved in H_2O/DMF (8 mL; v/v = 3:7). The solution was heated at 80 °C for 48 h in a sealed autoclave and cooled to 30 °C over 12 h to yield **KGF-31** as colorless needle-like crystals.

Pure **KGF-29** powder

The pure **KGF-29** powder was obtained using *o*-HSPhOMe monomers. $Cd(NO_3)_2 \cdot 4H_2O$ (18.5 mg, 0.06 mmol) and *o*-HSPhOMe (17.2 mg, 0.12 mmol) were dissolved in H_2O/DMF (2 mL; v/v = 1:9). The solution was heated at 60 °C for 48 h in a sealed autoclave and cooled to 30 °C over 12 h. The resulting white solid was collected by centrifugation (4000 rpm, 3 min), washed with acetone, and dried under vacuum to obtain pure **KGF-29** as a white powder. Yield: 13.6 mg (57.8 %). Anal. $CdS_2C_{14}H_{14}O_2$: calcd. C: 43.03, N: 0.00, H: 3.61; found. C: 43.04, N: 0.00, H: 3.47.

Pure **KGF-30** powder

$Cd(NO_3)_2 \cdot 4H_2O$ (92.5 mg, 0.3 mmol) and *m*-HSPhOMe (85.8 mg, 0.6 mmol) were dissolved in H_2O/DMF (8 mL; v/v = 1:1). The solution was heated at 80 °C for 48 h in a sealed autoclave and cooled to 30 °C over 12 h. The resulting white solid was collected by centrifugation (4000 rpm, 3 min), washed with acetone, and dried under vacuum to obtain pure **KGF-30** as a white powder. Yield: 84.7 mg (72.1 %). Anal. $CdS_2C_{14}H_{14}O_2$: calcd. C: 43.03, N: 0.00, H: 3.61; found. C: 42.87, N: 0.00, H: 3.15.

Pure **KGF-31** powder

$Cd(NO_3)_2 \cdot 4H_2O$ (92.5 mg, 0.3 mmol) and *p*-HSPhOMe (87.6 mg, 0.6 mmol) were dissolved in a mixture of H_2O and DMF (8 mL; v:v = 3:7). The solution was heated at 80 °C for 48 h in a sealed autoclave and cooled to 30 °C over 12 h. The resulting white solid was collected by centrifugation (4000 rpm, 3 min), washed with acetone, and dried under vacuum to obtain pure **KGF-31** as a white powder. Yield: 80.0 mg (68.1%). Anal. $CdS_2C_{14}H_{14}O_2 + 0.47H_2O$: calcd. C: 42.12, N: 0.00, H: 3.77; found. C: 41.85, N: 0.00, H: 3.47. The water molecule in the pure **KGF-31** powder may be derived from moisture.

Methods

Elemental analysis

Elemental analysis was performed at A-Rabbit-Science Japan Co., Ltd.

Single-crystal X-ray diffraction (SCXRD)

SCXRD patterns of **KGF-29** and **KGF-30** were collected using a Rigaku Saturn CCD diffractometer with Mo K_α radiation. The SCXRD pattern of **KGF-31** was collected using a Rigaku XtaLAB Synergy-S diffractometer equipped with a HyPix6000HE hybrid photon counting detector using Cu K_α radiation. The diffraction profiles were integrated using the CrysAlisPro software. Crystal structures were solved via direct methods using the SHELXT program and refined with SHELXL.[S2,S3] All non-H atoms were refined using anisotropic thermal parameters. All calculations were performed using the Olex2 crystallographic software package.[S4]

X-ray photoelectron spectroscopy (XPS)

XPS spectra were obtained using a JPS-9010MC, JEOL. The obtained data were calibrated using the binding energy of the Au 4f orbital.

Powder X-ray diffraction (PXRD)

PXRD patterns were collected using a Rigaku MiniFlex600 diffractometer operating at 40 kV and 15 mA with a Cu-target tube. Samples were examined without grinding, and data were collected in the diffraction angle (2θ) range of 2–50° using Cu K_α radiation. Simulated PXRD patterns were calculated using SCXRD data using the diffraction crystal module of the Mercury program.

Scanning electron microscopy (SEM) and energy-dispersive X-ray spectroscopy (EDX)

SEM textures and EDX maps were recorded on a JEOL JCM-6000 system equipped with an EDS analyzer (EX-37001) and a DX200s detector. All samples were sputter-coated with Au before analysis.

Thermogravimetry–differential scanning calorimetry (TG–DSC)

TG–DSC was performed with a HITACHI STA200RV instrument from 30–500 °C at a heating rate of 10 °C min^{-1} under N_2.

Diffuse-reflectance ultraviolet–visible (DR-UV–Vis) spectroscopy

DR-UV–Vis spectra (200–800 nm) were recorded with a Shimadzu UV-3600 UV–Vis–NIR spectrophotometer using $BaSO_4$ powder as a non-adsorbing background. The bandgaps were calculated by the Kubelka–Munk (KM) function using the following equation:

$$\frac{K}{S} = F(R) = \frac{(1-R)^2}{2R}$$

where K is the absorption coefficient, S is a scattering factor, R is the reflectance, and $F(R)$ is the KM function. The band gaps in **KGF-29** and **KGF-31** were determined from the Tauc plot of $[F(R) \times h\nu]^{1/2}\ vs.\ h\nu$ and that of **KGF-30** from the Tauc plot of $[F(R) \times h\nu]^{2}\ vs.\ h\nu$ by extrapolating the linear region to the abscissa.

Photoelectron yield spectroscopy (PYS)

Crystalline samples were placed on a conductive carbon tape on a glass substrate, which was connected to the earth wire in a vacuum chamber (10^{-4} Pa) of a Bunko Keiki BIP-KV202GD instrument. The sample was exposed to monochromated ultraviolet (UV) light (4–7 eV corresponding to 355 to 177 nm), and the photoelectrons emitted from the sample were detected. The photon number (power) of UV light was measured by a photodetector prior to the experiment.

Time-resolved microwave conductivity (TRMC)

Crystalline samples on an adhesive tape attached to a quartz substrate were placed in the resonant cavity and exposed to continuous microwave radiation at approximately 9.1 GHz. The third harmonic generation (355 nm) of a Nd:YAG laser (Continuum Inc., Surelite II, pulse duration = 5–8 ns, 10 Hz) was used as the excitation source (incident photon density $I_0 = 9.1 \times 10^{15}$ photons cm^{-2} pulse^{-1}). The photoconductivity ($\Delta\sigma = A^{-1}\ \Delta P_\text{r}\ P_\text{r}^{-1}$ where A is the sensitivity factor, P_r is the reflected microwave power, and ΔP_r is the change in P_r upon exposure to light) was converted into the product of the quantum yield (φ) and sum of the charge carrier mobilities $\Sigma\mu$ ($= \mu_+ + \mu_-$) using the relationship $\varphi\Sigma\mu$

$= \Delta\sigma(eI_0F_{\mathrm{light}})^{-1}$, where e and F_{Light} are the electron charge and correction (or filling) factor, respectively. The experiments were performed at 25 °C in air.

First-principles calculations

First-principles calculations were performed using CASTEP 2020 (20.1.0.5). The generalized gradient approximation (GGA) and the Perdew–Burke–Ernzerhof (PBE) exchange correlation potential with the ultrasoft pseudopotential plane-wave method were used. The plane-wave cut-offs were set to 630 eV for **KGF-29,** 490 eV for **KGF-30** and 630 eV for **KGF-31**. The Brillouin zones of **KGF-29**, **KGF-30**, and **KGF-31** were sampled with a $4 \times 3 \times 2$ k-point mesh, $2 \times 3 \times 6$ k-point mesh, and $2 \times 2 \times 1$ k-point mesh, respectively.

Table S1. Crystallographic data for **KGF-29**, **KGF-30**, and **KGF-31**.

Compound	**KGF-29**	**KGF-30**	**KGF-31**
Formula	$C_{14}H_{14}CdO_2S_2$	$C_{14}H_{14}CdO_2S_2$	$C_{14}H_{14}CdO_2S_2$
Formula weight	390.77	390.77	390.81
T / K	150	150	293
Crystal system	Triclinic	Orthorhombic	Orthorhombic
Space group	$P\bar{1}$	$Pccn$	$Iba2$
a / Å	6.8847(3)	28.1725(6)	35.4206(10)
b / Å	8.4110(3)	13.9425(3)	16.8187(4)
c / Å	12.8724(4)	7.0402(2)	7.2759(2)
α / °	92.960(3)	90	90
β / °	101.422(3)	90	90
γ / °	105.459(3)	90	90
V / Å^3	699.89(5)	2765.36(11)	4334.5(2)
Z	2	8	12
R_1 ($I > 2\sigma(I)$)	0.0233	0.0278	0.0432
R_1 (all data)	0.0287	0.0290	0.0609
wR_2 ($I > 2\sigma(I)$)	0.0559	0.0698	0.1080
wR_2 (all data)	0.0550	0.0702	0.1196
GOF	1.054	1.247	1.003
Flack	–	–	0.02(2)
CCDC number	2306984	2307085	2306985

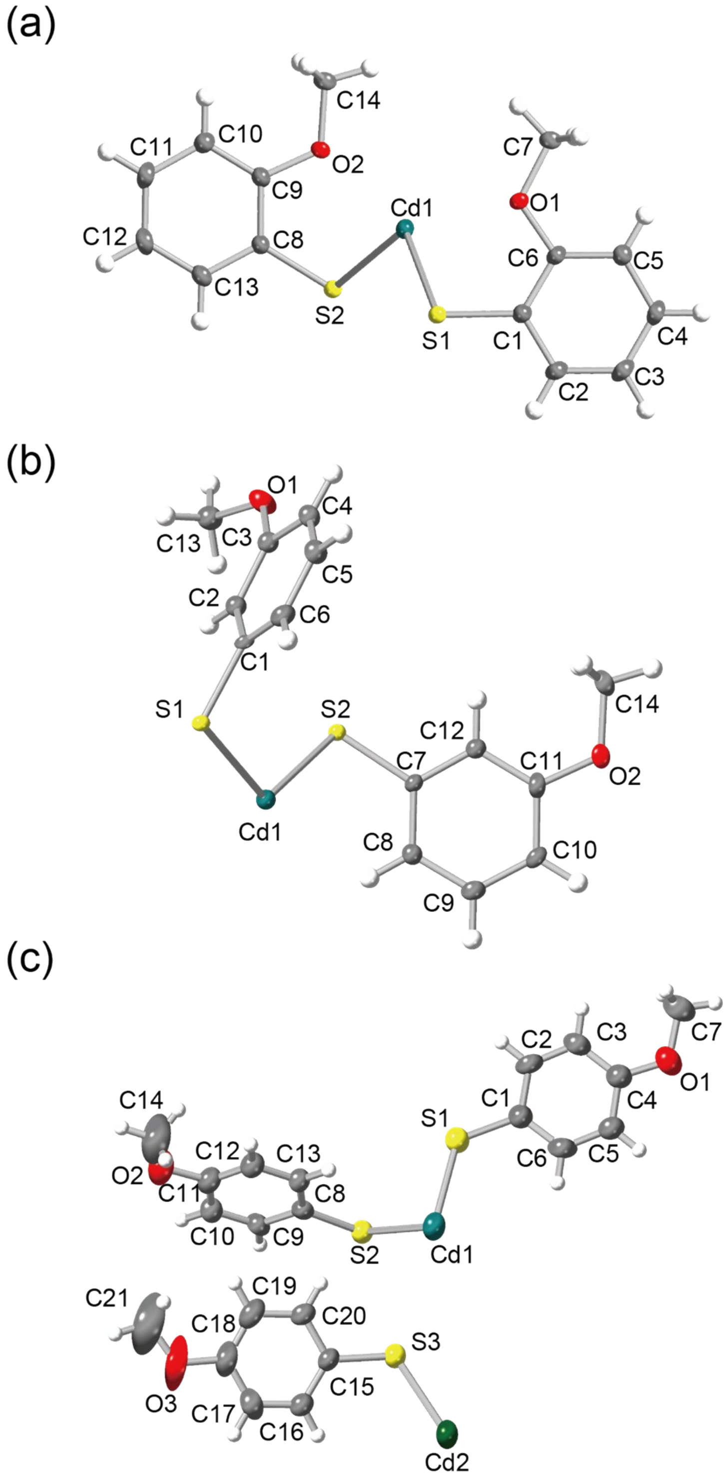

Fig. S1. Asymmetric units of (a) **KGF-29**, (b) **KGF-30**, and (c) **KGF-31** depicted at 50% thermal ellipsoid probability.

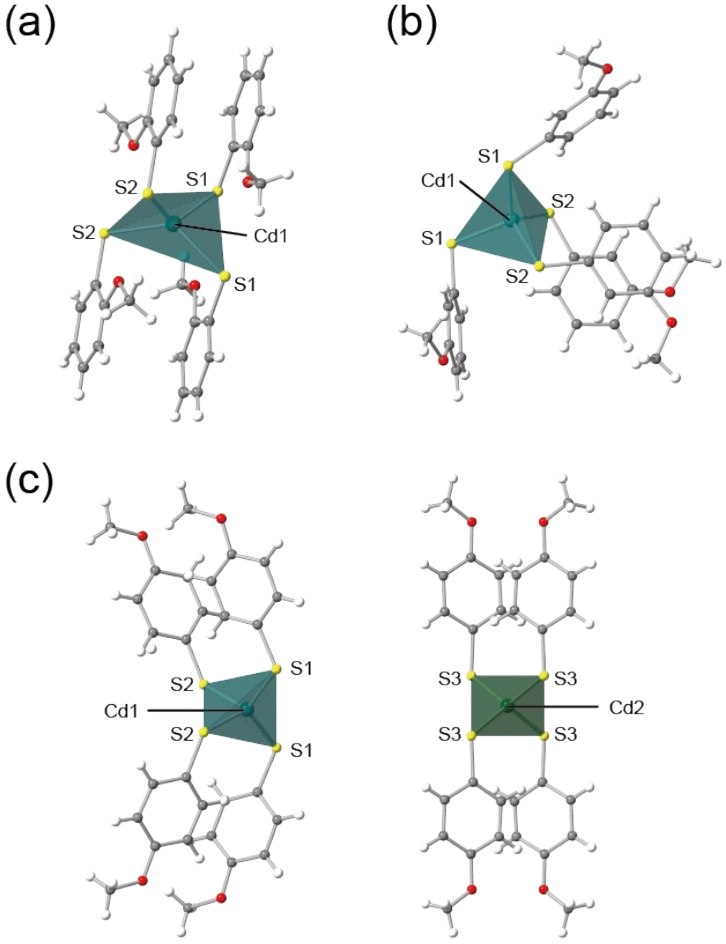

Fig. S2. Coordination structure around Cd(II) ion of (a) **KGF-29**, (b) **KGF-30**, and (c) **KGF-31**.

Table S2. Selected bond distances (Å) in **KGF-29, KGF-30, KGF-31**, and CdS.

Bond	**KGF-29**	**KGF-30**	**KGF-31**	*α*-CdS	*β*-CdS
Cd1–S1	2.584	2.589	2.545	2.526	2.502
Cd1–S1	2.597	2.593	2.602	2.540	2.502
Cd1–S2	2.600	2.561	2.569	2.540	2.502
Cd1–S2	2.601	2.562	2.579	2.540	2.502
Cd2–S3	–	–	2.563	–	–
Cd2–S3	–	–	2.563	–	–
Cd2–S3	–	–	2.572	–	–
Cd2–S3	–	–	2.572	–	–
Cd1-S ave.	2.600	2.576	2.574	2.537	2.502
Cd2-S ave.	–	–	2.568	–	–

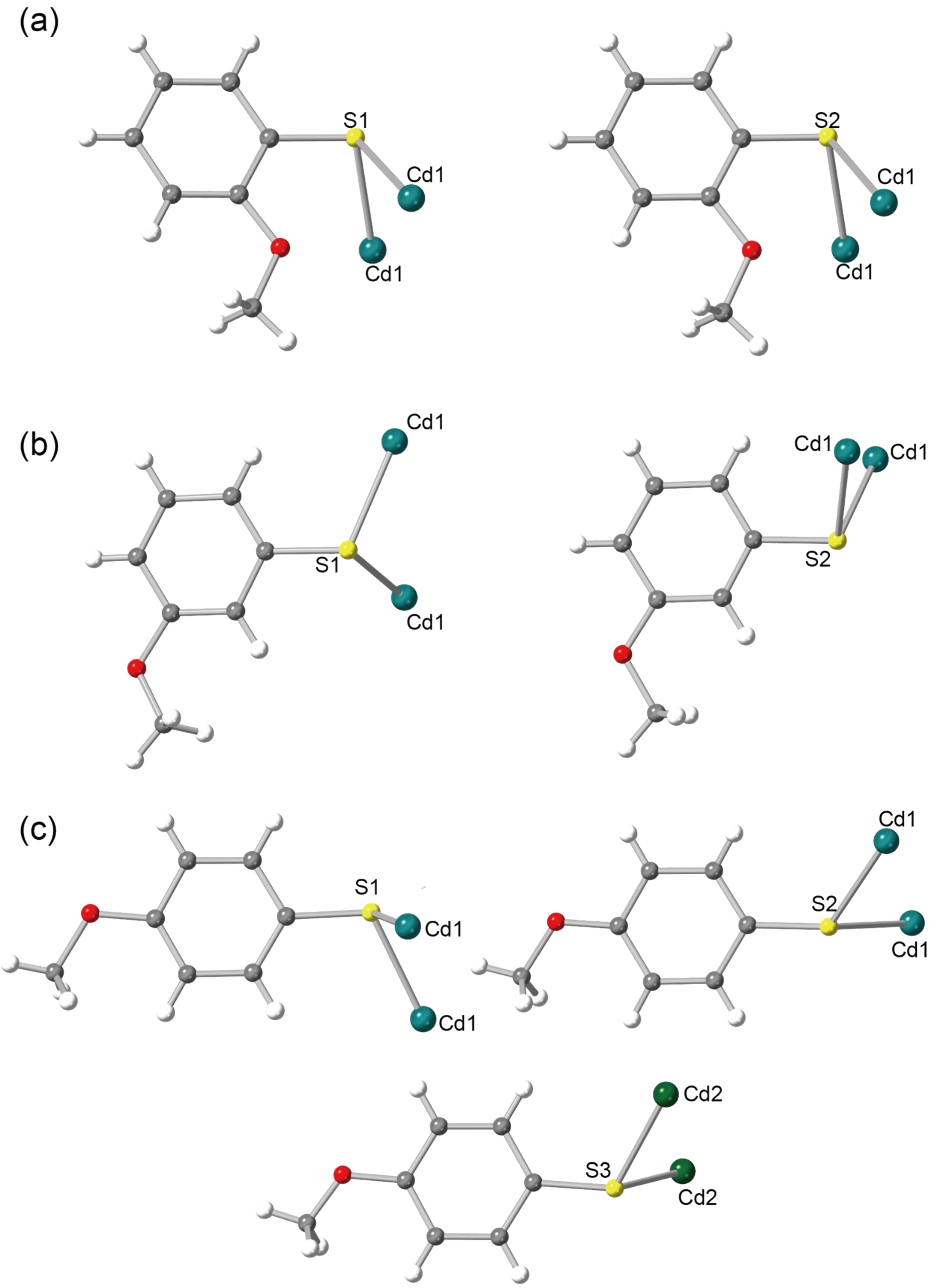

Fig. S3. Coordination mode of SPhOMe^- anions in (a) **KGF-29**, (b) **KGF-30**, and (c) **KGF-31**.

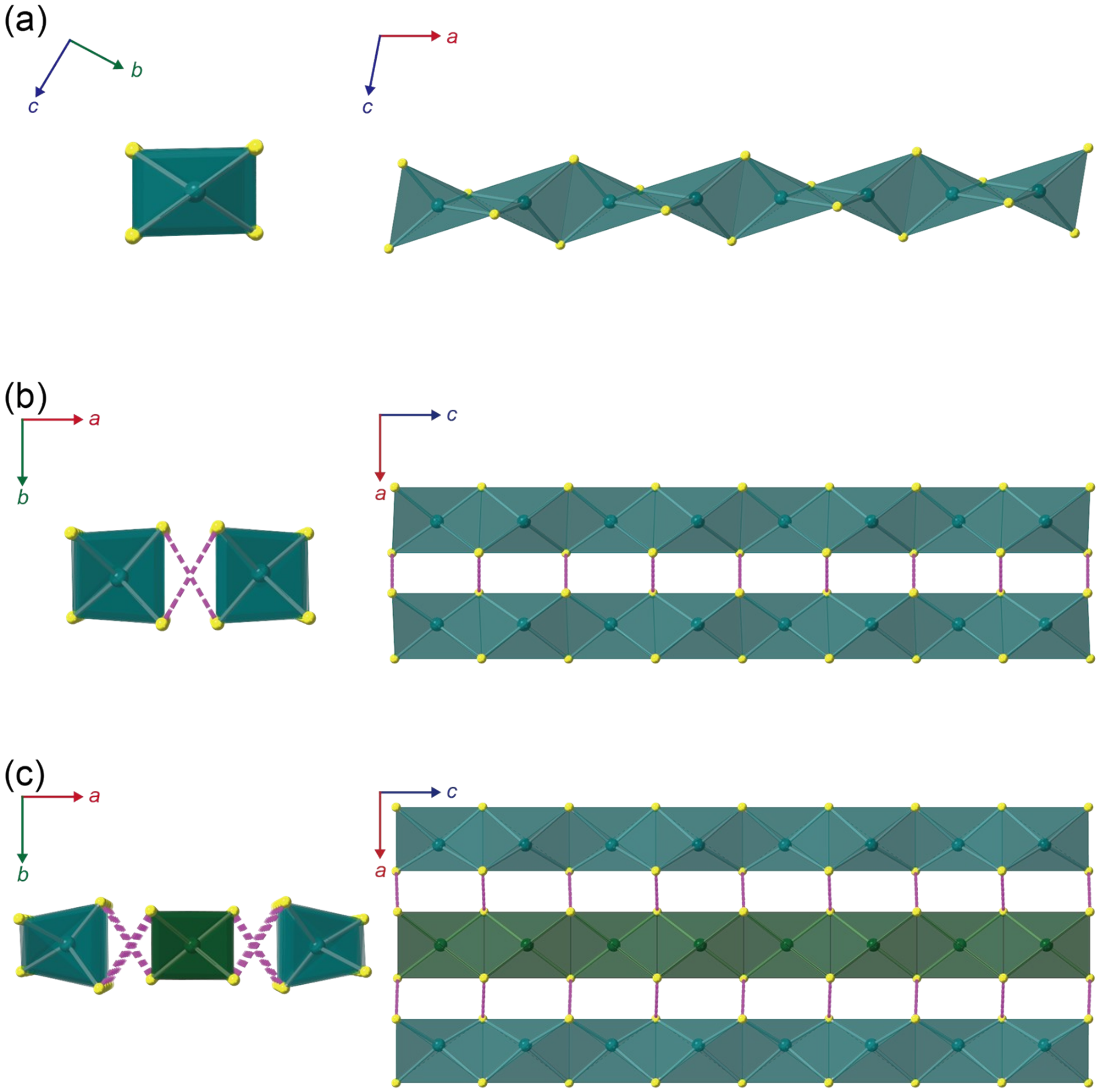

Fig. S4. Inorganic (–Cd–S–)$_n$ structures in (a) **KGF-29**, (b) **KGF-30**, and (c) **KGF-31**. S···S interchain interactions are colored in purple.

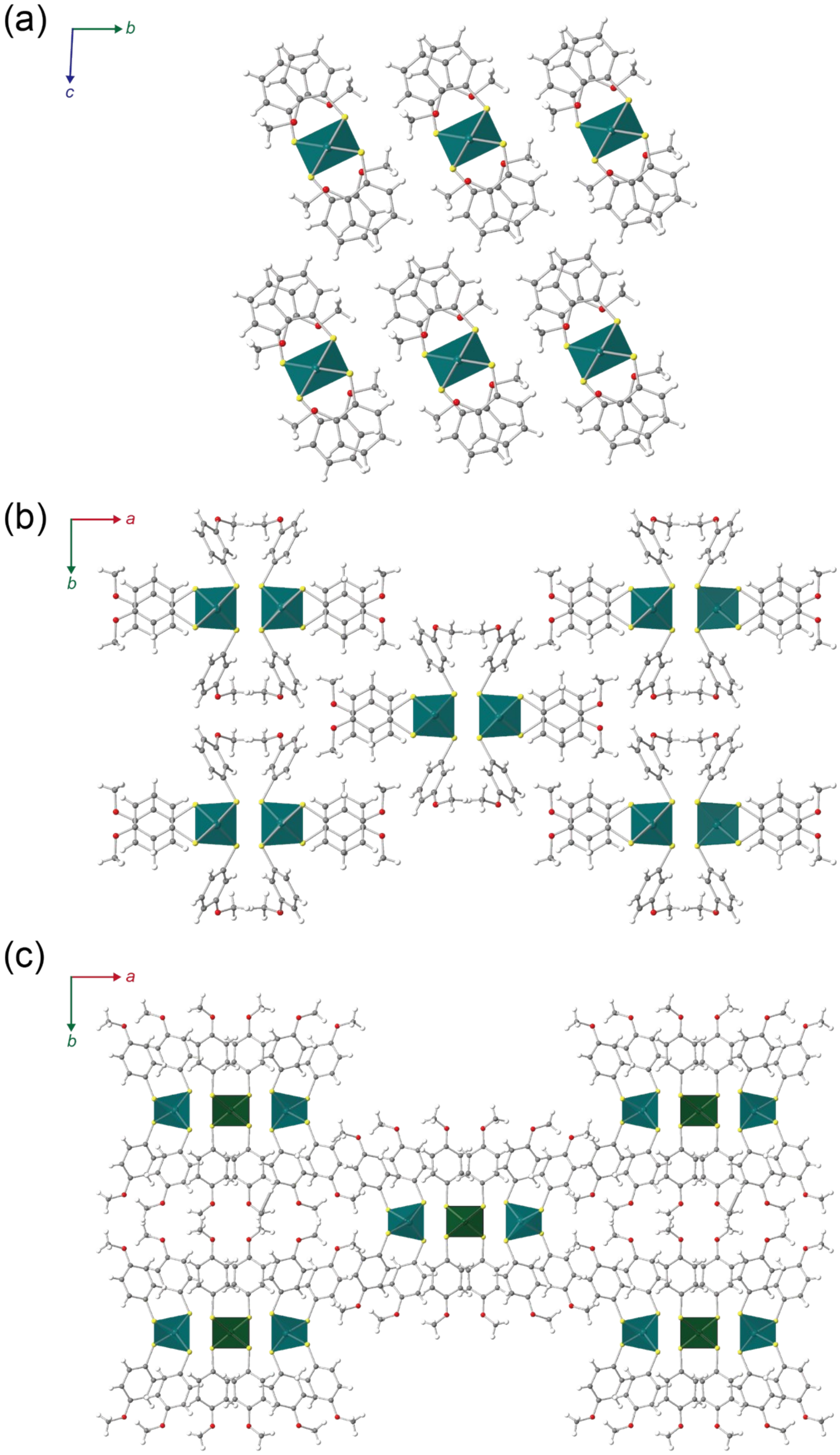

Fig. S5. Packing structures of (a) **KGF-29**, (b) **KGF-30**, and (c) **KGF-31**.

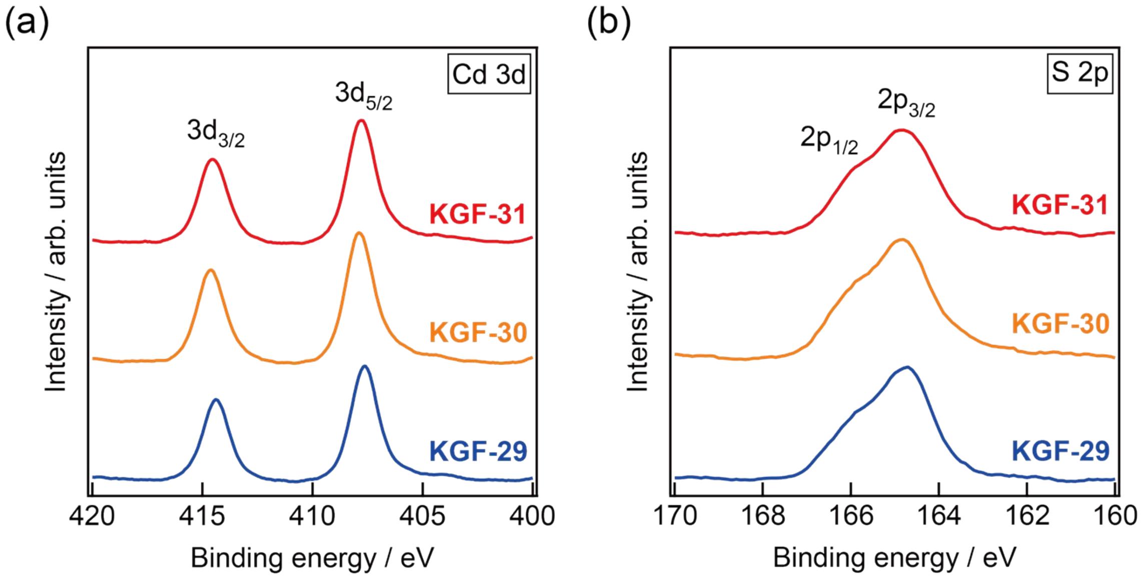

Fig. S6. XPS results of **KGF-29**, **KGF-30**, and **KGF-31**. (a) Cd 3d and (b) S 2p spectra.

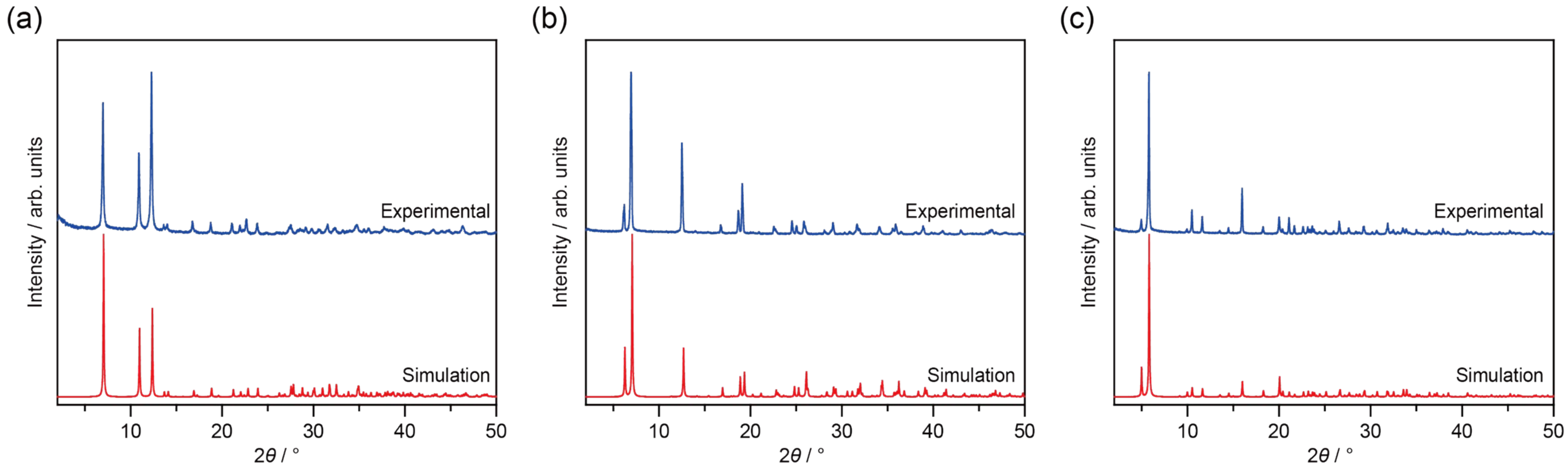

Fig. S7. PXRD patterns of (a) **KGF-29**, (b) **KGF-30**, and (c) **KGF-31** (the simulated pattern was obtained from single-crystal X-ray structural analysis).

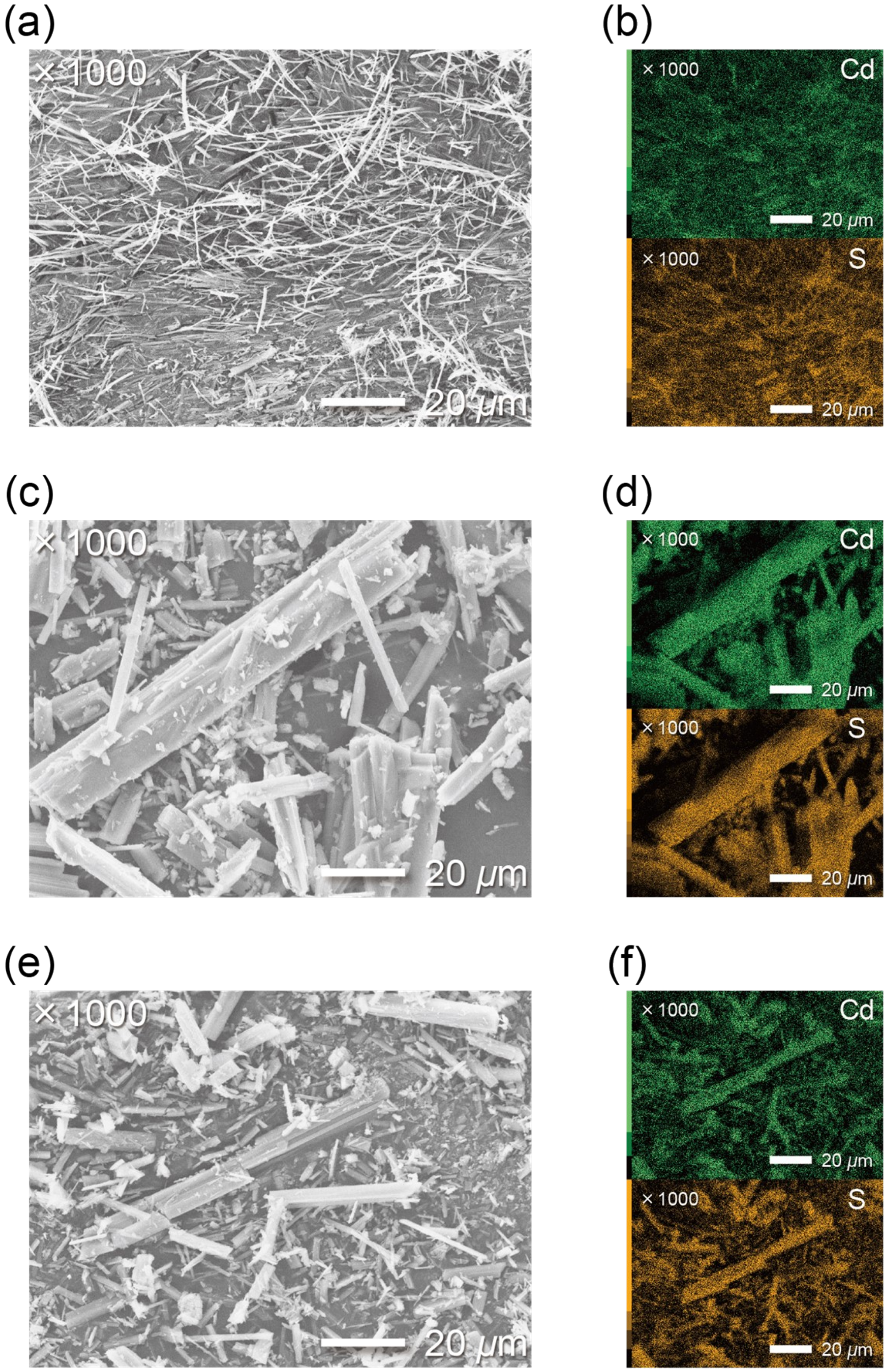

Fig. S8. SEM images of (a) **KGF-29**, (c) **KGF-30**, and (e) **KGF-31** and EDS maps of (b) **KGF-29**, (d) **KGF-30**, and (f) **KGF-31.** The Cd/S ratios of **KGF-29**, **KGF-30**, and **KGF-31** are 1/1.8, 1/1.7, and 1.1/7, respectively.

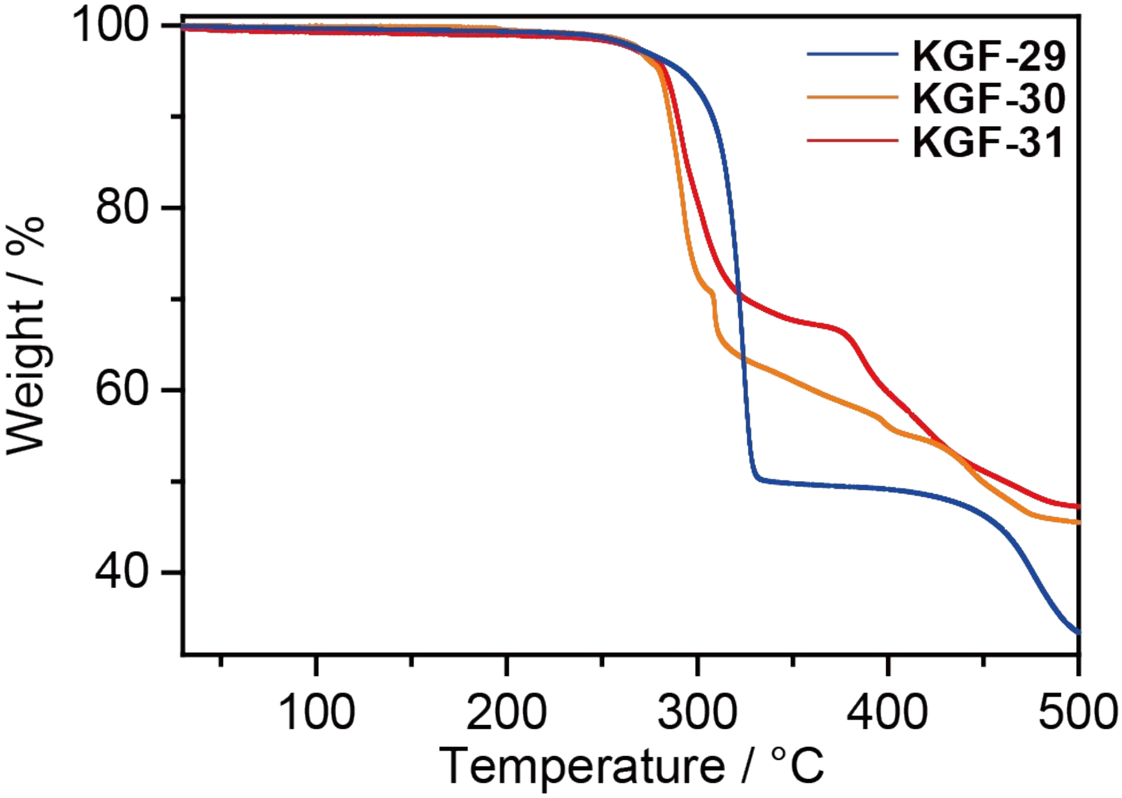

Fig. S9. TG curves of **KGF-29** (blue), **KGF-30** (orange), and **KGF-31** (red).

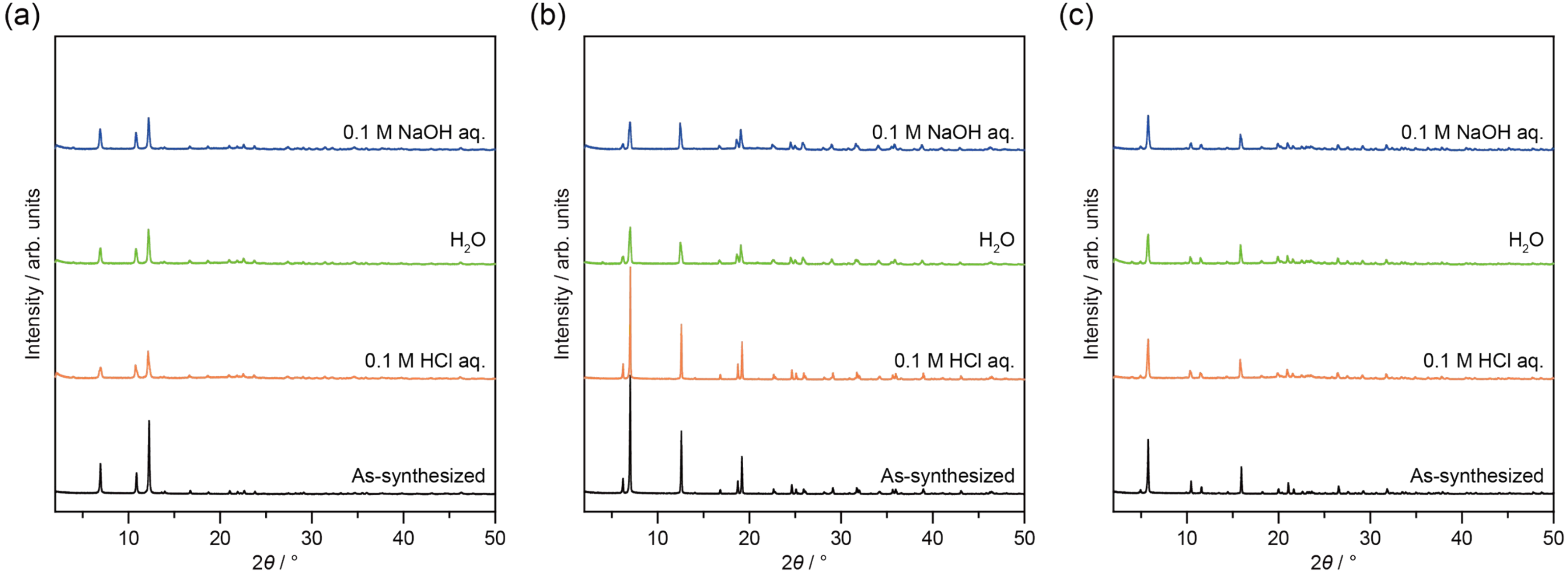

Fig. S10. Chemical stabilities of (a) **KGF-29**, (b) **KGF-30**, and (c) **KGF-31** toward H_2O, 0.1 M HCl, and 0.1 M NaOH.

Table S3. Summary of direct and indirect band gap energies of **KGF-29**, **KGF-30**, and **KGF-31**.

	KGF-29	**KGF-30**	**KGF-31**
Direct band gap	3.99 eV	3.77 eV	3.41 eV
Indirect band gap	3.75 eV	3.50 eV	3.19 eV

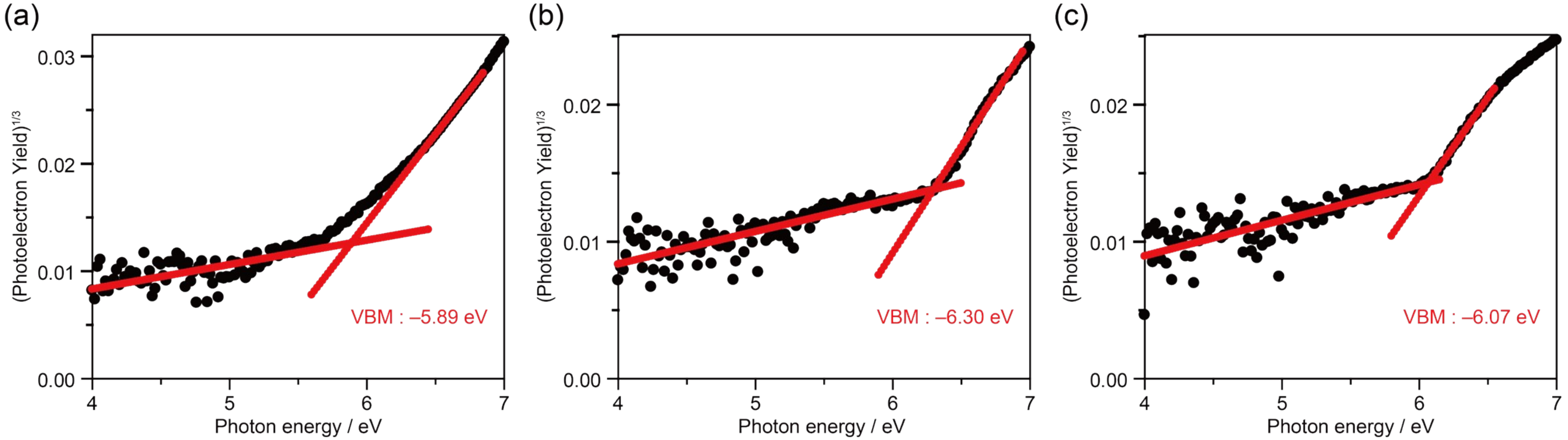

Fig. S11. PYS analyses of (a) **KGF-29**, (b) **KGF-30**, and (c) **KGF-31**.

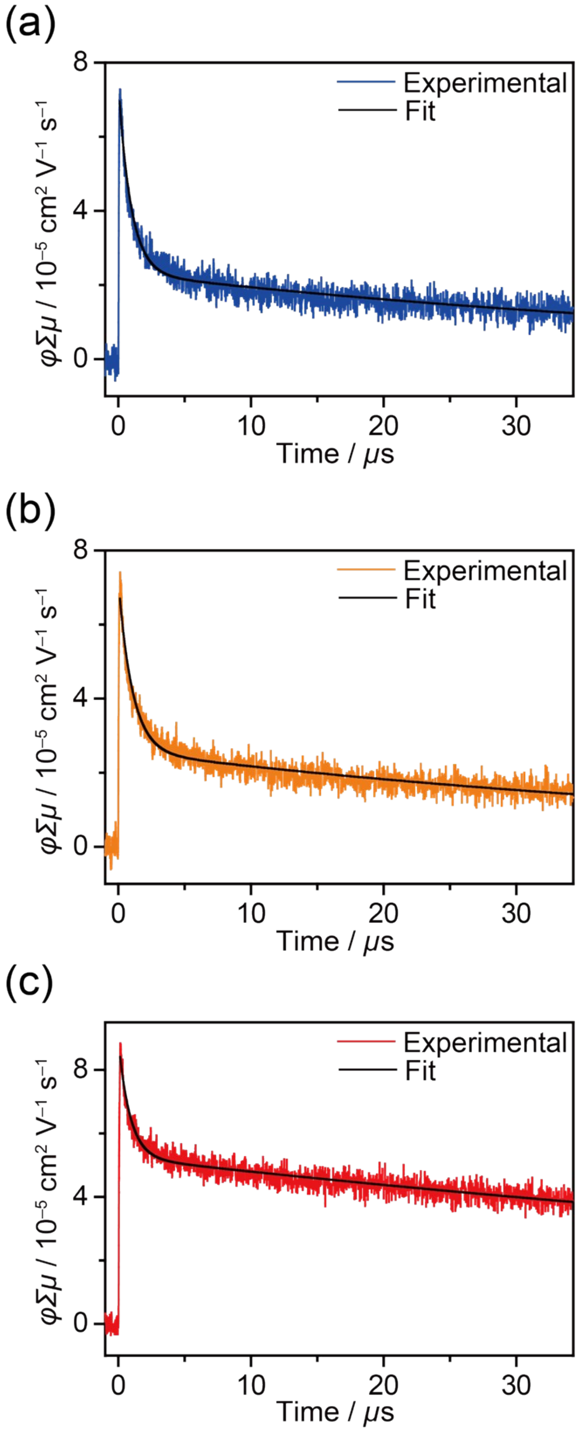

Fig. S12. TRMC decays and exponential fitting of (a) **KGF-29**, (b) **KGF-30**, and (c) **KGF-31**.

Table S4. TRMC results obtained for photoconductive coordination polymers and metal-organic frameworks.

Compound	$\varphi\Sigma\mu$ / cm^2 V^{-1} s^{-1}	Reference
$[Pb_3ttc_2 \cdot 2H_2O]_n$	7.4×10^{-5}	S5
$[Pb(tadt)]_n$	4.9×10^{-5}	S6
$[Sn_2(Httc)_2 \cdot MeOH]_n$	1.8×10^{-5}	S7
$[Ag_2Httc]_n$	2.7×10^{-5}	S8
$[AgH_2ttc]_n$	2.8×10^{-5}	S8
$[Ag_3ttc]_n$	1.5×10^{-4}	S8
$[Ag(tzdt)]_n$	3.6×10^{-5}	S9
$[Ag_2(tzdt)(TFA)]_n$	2.2×10^{-5}	S9
$Mn_2(DSBDC)$	1.8×10^{-5}	S10
$Cu_4^ICu_2^{II}Br_4(pyr\text{-}dtc)_4$	3.0×10^{-5}	S11
$[Cd(o\text{-}SPhOMe)_2]_n$ (**KGF-29**)	7.3×10^{-5}	This work
$[Cd(m\text{-}SPhOMe)_2]_n$ (**KGF-30**)	7.4×10^{-5}	This work
$[Cd(p\text{-}SPhOMe)_2]_n$ (**KGF-31**)	8.8×10^{-5}	This work

Table S5. PDOS ratio (%) of **KGF-29**, **KGF-30**, and **KGF-31**

Element	**KGF-29**		**KGF-30**		**KGF-31**	
	HOMO	LUMO	HOMO	LUMO	HOMO	LUMO
Cd	4.8	22.6	2.6	51.8	4.0	68.7
S	43.0	3.4	29.3	18.9	35.4	24.0
C	45.3	66.0	53.7	28.4	45.6	9.54
O	5.8	1.2	12.1	0.6	12.5	0.3

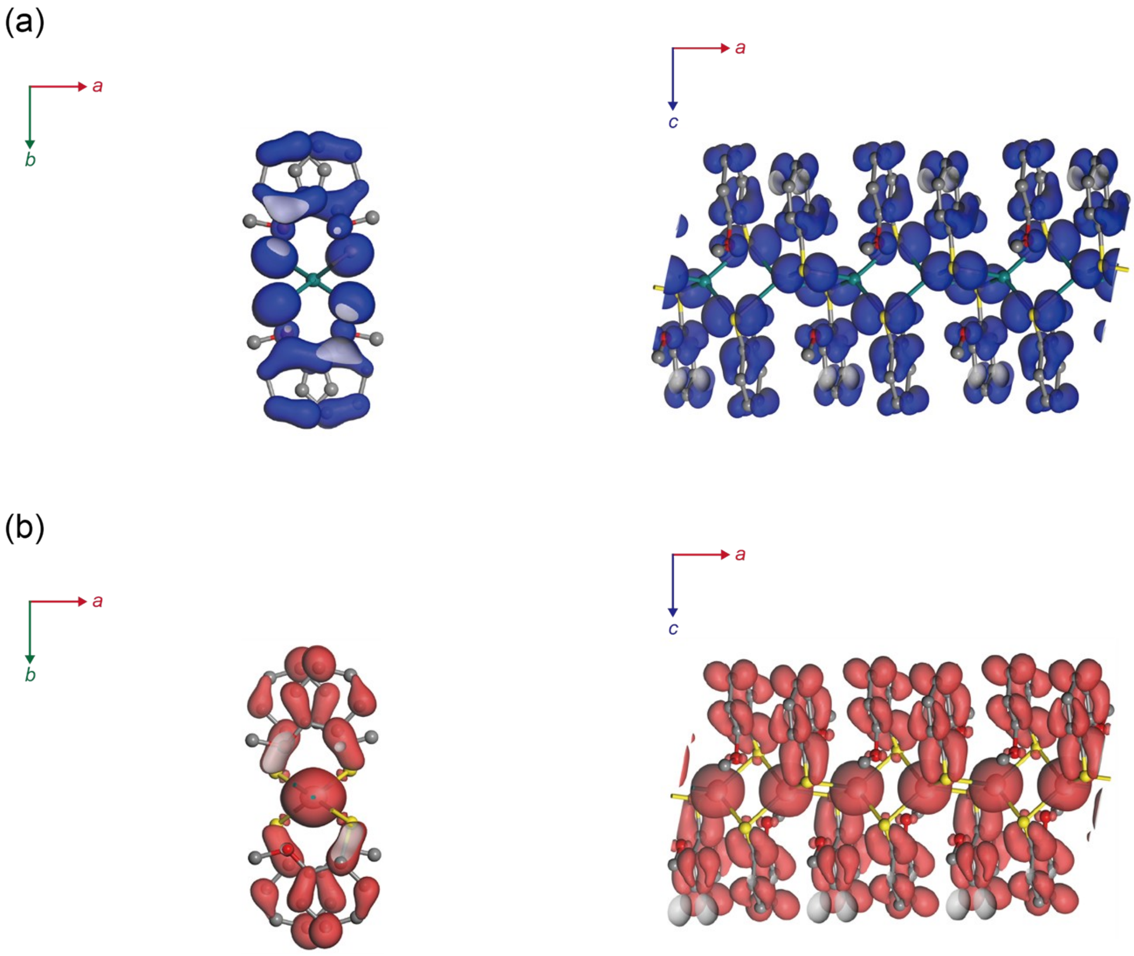

Fig. S13. (a) VBM and (b) CBM distributions of **KGF-29**.

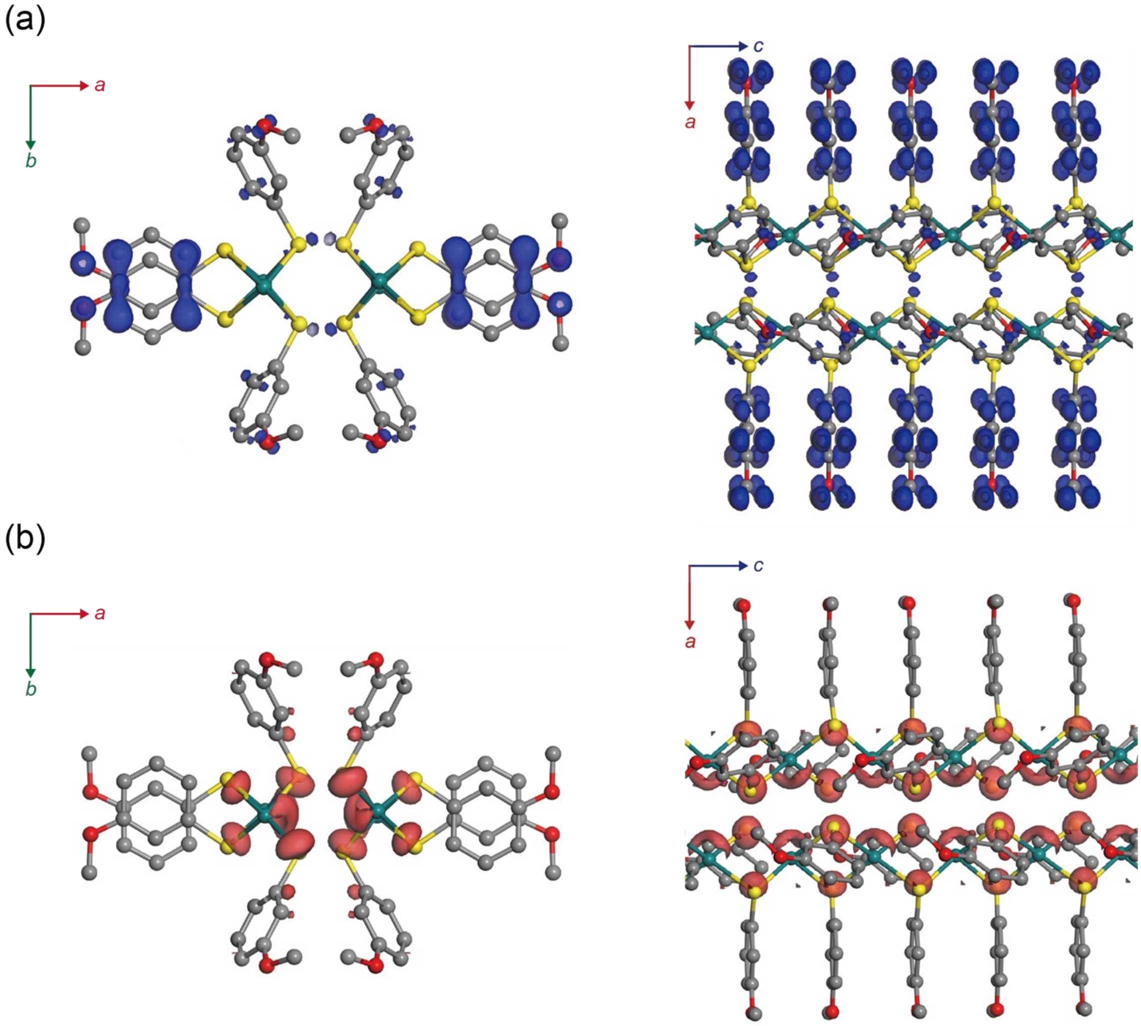

Fig. S14. (a) VBM and (b) CBM distributions of **KGF-30**.

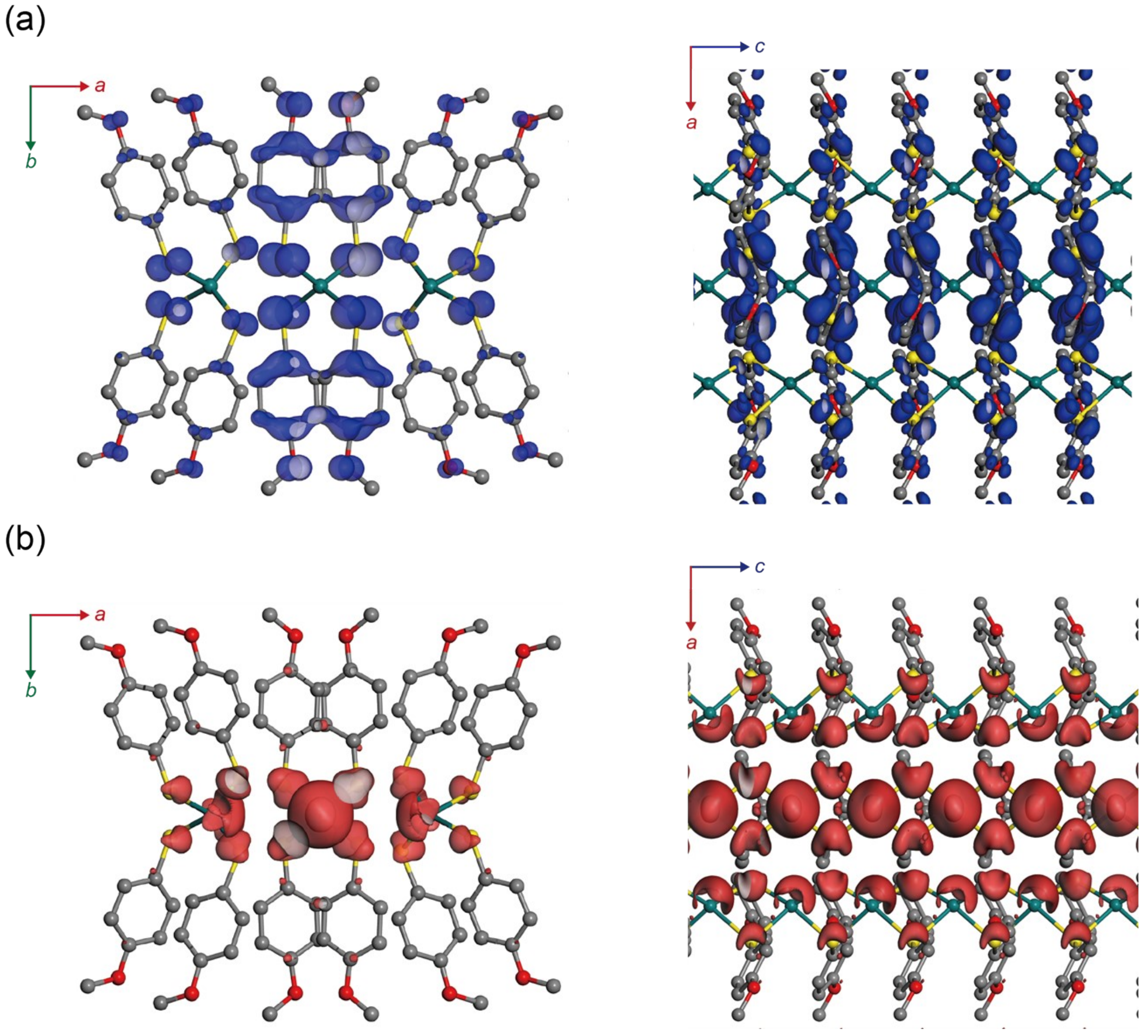

Fig. S15. (a) VBM and (b) CBM distributions of **KGF-31**.

References

S1. W. Paritmongkol, T. Sakurada, W. S. Lee, R. Wan, P. Müller and W. A. Tisdale, *J. Am. Chem. Soc.*, 2021, **143**, 20256.

S2. G. M. Sheldrick, *Acta Cryst.*, 2014, **A70**, C1437.

S3. G. M. Sheldrick, *Acta Cryst.*, 2008, **A64**, 112.

S4. O. V. Dolomanov, L. J. Bourhis, R. J. Gildea, J. A. K. Howard and H. Puschmann, *J. Appl. Crystallogr.*, 2009, **42**, 339.

S5. Y. Kamakura, P. Chinapang, S. Masaoka, A. Saeki, K. Ogasawara, S. R. Nishitani, H. Yoshikawa, T. Katayama, N. Tamai, K. Sugimoto, K. Sugimoto and D. Tanaka, *J. Am. Chem. Soc.,* 2020, **142**, 27.

S6. Y. Kamakura, C. Sakura, A. Saeki, S. Masaoka, A. Fukui, D. Kiriya, K. Ogasawara, H. Yoshikawa and D. Tanaka, *Inorg. Chem.,* 2021, **60**, 5436.

S7. Y. Kamakura, S. Fujisawa, K. Takahashi, H. Toshima, Y. Nakatani, H. Yoshikawa, A. Saeki, K. Ogasawara and D. Tanaka, *Inorg. Chem.,* 2021, **60**, 12691.

S8. T. Wakiya, Y. Kamakura, H. Shibahara, K. Ogasawara, A. Saeki, R. Nishikubo, A. Inokuchi, H. Yoshikawa and D. Tanaka, *Angew. Chem. Int. Ed.,* 2021, **60**, 23217.

S9. R. Akiyoshi, A. Saeki, K. Ogasawara, H. Yoshikawa, Y. Nakamura and D. Tanaka, *CrystEngComm*, 2023, **25**, 2990.

S10. L. Sun, T. Miyakai, S. Seki, M. Dinca, *J. Am. Chem. Soc.,* 2013, **135**, 8185.

S11. T. Okubo, H. Anma, N. Tanaka, K. Himoto, S. Seki, A. Saeki, M. Maekawa and T. Kuroda-Sowa, *Chem. Commun,* 2013, **49**, 4316.